JACS
JOURNAL OF THE AMERICAN CHEMICAL SOCIETY

COMMUNICATION

pubs.acs.org/JACS

Ultrathin Gold Nanoframes through Surfactant-Free Templating of Faceted Pentagonal Silver Nanoparticles

Matthew McEachran,[†] Dilyn Keogh,[†] Brendan Pietrobon,[†] Nicole Cathcart,[†] Ilya Gourevich,[‡] Neil Coombs,[‡] and Vladimir Kitaev*[,†]

[†]Chemistry Department, Wilfrid Laurier University, 75 University Avenue West, Waterloo, Ontario, Canada N2L 3C5

[‡]Centre for Nanostructure Imaging, Chemistry Department, University of Toronto, 80 St. George Street, Toronto, Ontario, Canada M5S 3H6

Supporting Information

ABSTRACT: Ultrathin gold nanoframes (up to 1.6 nm) were prepared via templating upon well-defined faceted silver morphologies. Starting with silver decahedra, small quantities of gold (1−10 mol % relative to the amount of silver) were selectively deposited on the nanoparticle edges under optimized reducing conditions. Silver dissolution in hydrogen peroxide yielded well-defined gold frames that retained their structural integrity in the ultrathin nanowire regime below 2 nm. The frame formation protocol was also successfully applied to other silver nanoparticle shapes featuring pentagonal twinning and (111) facets (e.g., pentagonal faceted rods and icosahedra). The demonstrated approach can be applied in the controlled preparation of ultrathin metal nanowires complementary to lithography and in the production of ultrafine noble-metal nanostructures for catalytic applications.

Metal nanoparticles[1,2] and nanostructures[3] have become an established research field because of their advantageous properties in plasmonics,[4] sensing,[5] medical applications,[6,7] and catalysis.[8,9] Gold nanoparticles in particular have received considerable attention because of their versatility and chemical stability. At the same time, the inertness of gold causes appreciable challenges in shape control of gold nanoparticles[10] in comparison with more reactive metals such as silver.[1] Consequently, templating of silver morphologies with gold has been pioneered by the Xia group, who achieved versatile shape and size control[11] and at the same time opened the way to new classes of hollow gold nanostructures: cages,[12] rattles,[13] frames,[14] etc. Substantial research efforts have been recently invested in the templated synthesis of gold nanostructures using different silver morphologies[15] and deposition procedures[16] and in studies of the optical properties and applications of these nanostructures in plasmonics[17] and surface-enhanced Raman scattering (SERS).[18]

Templating as a selective deposition process is akin to lithography, and although it may be challenging for colloidal chemistry to compete with the recent advances in controlled formation of hollow functional structures,[19] the following question arises: what is the finest structural feature that can be produced by selective gold deposition onto silver nanoparticles with well-defined shapes? The interest in such fine nanostructures is further highlighted by recent developments in ultrathin nanowires[20] and, in particular, ultrathin gold nanowires,[21] given their advantageous properties in catalysis and similarities to superatomic gold clusters.[22] No systematic studies of ultrathin gold nanoframes have been reported to date.

Herein we demonstrate that selective gold deposition onto decahedral silver nanoparticles under optimized reducing conditions and subsequent silver etching offers a reliable pathway to well-defined gold nanoframes. Through control of the amount of the deposited gold, the thickness of the nanoframe skeleton can be tuned from ca. 5 to 1.6 nm, reaching the size domain of ultrathin nanowires, with the preservation of its structural integrity.[21] The frame formation was also applied to the (111) facets of pentagonal silver rods and icosahedra and therefore can serve as a general synthetic approach to ultrathin nanostructures with controlled dimensions.

Decahedral (Johnson solid J_{13}) silver nanoparticles[23] (AgNPs) were selected as a primary template morphology for gold deposition because of their good size monodispersity, shape selectivity, and, most importantly, well-defined edges connecting 10 (111) facets of the decahedron (Figure 1a). Through systematic variation of the reducing agent and its concentration, the pH, the amount of gold, and the rate of gold addition, we attained conditions for selective deposition of gold at the edges of the decahedra that subsequently remained as a thin continuous gold frame upon removal of the silver, as shown in Figures 1 and 2.

Ascorbic acid (AA), a common reducing agent for gold regrowth,[24] was found to work optimally in large excess (4.8 mM vs 0.002−0.03 mM deposited gold) for continuity and integrity of the resulting frames. Stronger reducing agents displayed a tendency to partially reduce gold in solution (rather than exclusively on the surface of the AgNPs), thus interfering with the selective deposition. The deposition was best performed at the pH of 8−9 produced by the trisodium citrate present in the original AgNP solution as a charge stabilizer and AA used in the form of sodium ascorbate. Using large concentrations of AA in a weakly alkaline solution (where AA is a strong reducing agent by the nature of its pH-dependent redox potential) was important for maximally counteracting the dissolution of silver through the fast process of galvanic replacement.[26] In more basic solutions (upon addition of a strong base), the gold deposition proceeded more slowly, and the selectivity of the deposition onto the polyhedra edges was lost, resulting in more uniform plating and formation of shells instead of frames. Overall, the selected

Received: December 26, 2010
Published: May 10, 2011

dx.doi.org/10.1021/ja111642d | J. Am. Chem. Soc. 2011, 133, 8066–8069

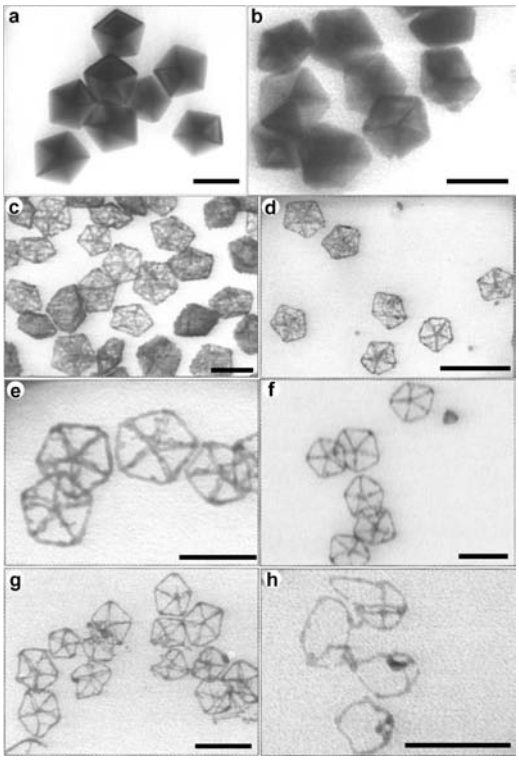

Figure 1. TEM images illustrating the formation of gold nanoframes and nanocages upon deposition of gold onto decahedral AgNPs and subsequent silver dissolution with hydrogen peroxide. (a) Silver decahedra prior to gold deposition. (b) Decahedra after deposition of gold (10 mol % relative to silver). (c–h) Images of the frames and cages after dissolution of silver with hydrogen peroxide. The amounts of gold deposited relative to silver in the template AgNPs were 20, 15, 7, 5, 3, and 1 mol %, respectively. All scale bars are 50 nm.

conditions afforded more selective and smooth gold deposition with cleaner edges of the resulting frames, as demonstrated in Figure 1b. The rate of the addition of gold precursor (tetrachloroauric acid) was found to be crucial for the frame integrity. A gold addition rate of 5%$_{Au/Ag}$ per minute (where X%$_{Au/Ag}$ represents X mol % gold relative to the silver present in the template AgNPs) proved to be optimal, as shown in Figure S1a,b in the Supporting Information. In a typical run performed using 3.0 mL of AgNPs at a silver concentration of 0.12 mM, tetrachloroauric acid was added at a rate of 1.8×10^{-8} mol/min (or 0.36 mL/min for a 5.0×10^{-5} M solution of $HAuCl_4$) to increase the gold concentration in solution by 0.006 mM/min.

Lower deposition rates caused a nonuniform gold distribution, with some frames becoming thicker as a result of preferred gold deposition (Figure S1c,d). Higher rates resulted in more grainy and rougher frames, likely as a result of increased galvanic replacement relative to gold reduction by AA and corresponding corrosion of the silver template (Figure S1e,f).

The deposition of up to ca. 15%$_{Au/Ag}$ under the optimized conditions resulted in smooth, uniform structures with excellent preservation of the original decahedral morphology, as confirmed by transmission electron microscopy (TEM) (Figure 1b). At the same time, the deposited gold could be qualitatively detected by energy-dispersive X-ray spectroscopy (EDX), and gold deposition had a pronounced effect on the plasmon absorption as monitored by UV–vis spectroscopy (Figure S2).

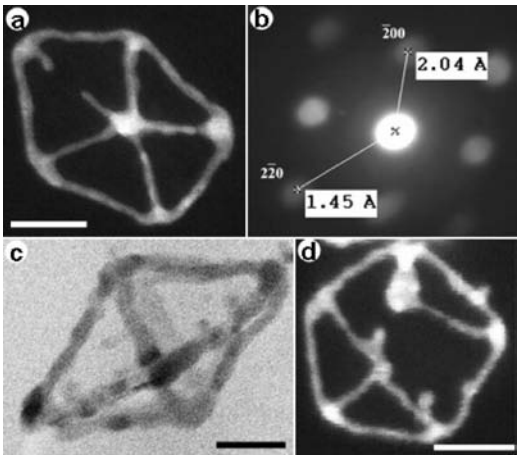

Figure 2. (a, c, d) High-resolution scanning TEM (STEM) images of gold frames. The amount of gold deposited relative to the silver in the template AgNPs was (a) 2 and (c, d) 3 mol %. (b) STEM nanodiffraction pattern for the sample shown in (a). All scale bars are 20 nm.

The selectivity of the gold deposition onto the edges and vertices was corroborated by the disappearance of the transverse plasmonic mode (along the shorter dimension of the decahedron along the C_5 axis) at 410 nm with less than 1.5%$_{Au/Ag}$ deposited onto the edges of the silver decahedra, while the main plasmonic peak (λ_{max}) at 490 nm was barely affected. Upon the deposition of up to 30%$_{Au/Ag}$, the width of the decahedra increased by less than 10%, which would be responsible for a shift of λ_{max} only from 490 to ca. 505 nm in the case of pure silver deposition in decahedra regrowth.[23] Thus, the continuous shift of λ_{max} up to 560 nm upon gold deposition can be interpreted as the effective averaging of gold and silver plasmon resonances over a surface layer with a thickness of <5 nm.[25] A graph of λ_{max} versus the amount of the deposited gold showed a smooth, continuous increase with saturation at 20%$_{Au/Ag}$ (Figure S3). Incidentally, as 20%$_{Au/Ag}$ was approached, erosion of the deposited structures and the roughness of the resulting frames started to become noticeable (Figure 1c,d). Thus, the contribution of galvanic replacement (in addition to gold reduction by AA at the silver surface) cannot be fully excluded even at lower X%$_{Au/Ag}$ because of its fast kinetics.[26]

Dissolution of the silver from the gold-coated decahedra was accomplished using hydrogen peroxide as a clean and effective silver etchant.[5,27] Dissolution with Fe^{3+} and ammonia[28] was also tested for comparative purposes and produced frames that were similar but somewhat inferior in smoothness. The dissolution proceeded rapidly (less than 6 min to remove the silver at a peroxide concentration of 0.1 M), and the process was easily followed and documented by UV–vis spectroscopy (Figure S4). For the larger amounts of deposited gold (>15%$_{Au/Ag}$), silver dissolution yielded porous shells with some gold retained at both the facets and the edges (Figure 1c,d). In view of the higher selectivity for deposition at the edges, with progressive decreases in the amount of gold, a point could be reached (at ca. 9–10%$_{Au/Ag}$) where gold remained predominantly as the frame upon silver dissolution (Figures 1e–h and 3). Importantly, upon further decreases in the amount of the deposited gold, the frames preserved their structural integrity and decreased in both the size (relative to the original decahedra) and thickness of the frame skeleton (Figures 1 and 3b). When the amount of the

dx.doi.org/10.1021/ja111642d | J. Am. Chem. Soc. 2011, 133, 8066–8069

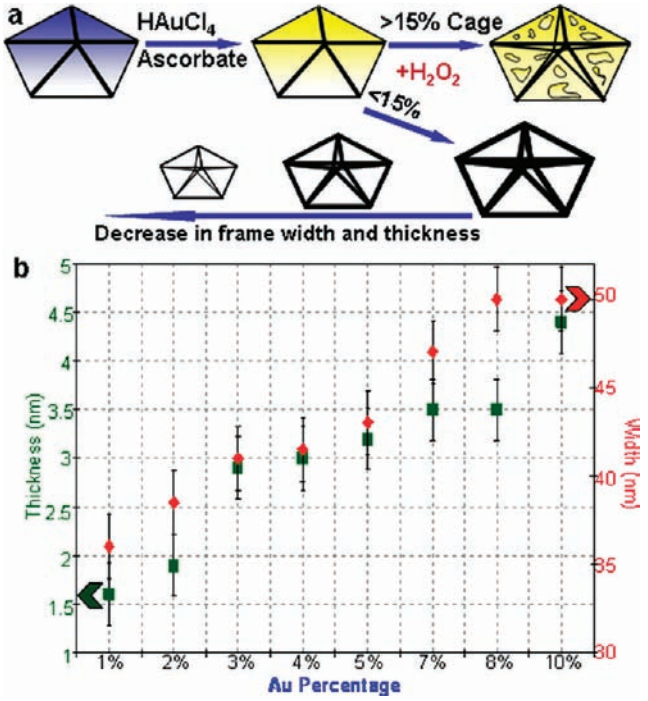

Figure 3. (a) Schematics of the formation of gold nanoframes templated from silver decahedra. (b) Dimensions of the resulting nanoframes (width on the right and thickness of the skeleton on the left) plotted as functions of the amount of deposited gold.

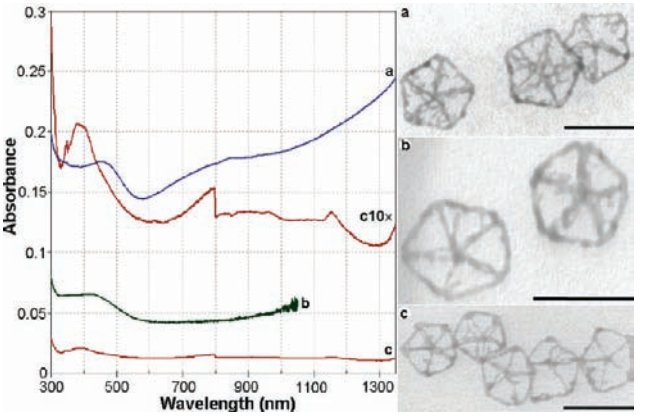

Figure 4. (left) UV−vis−NIR spectra of aqueous dispersions of Au frames prepared at different $X\%_{Au/Ag}$ after subsequent silver removal: (a) $7\%_{Au/Ag}$; (b) $3\%_{Au/Ag}$; (c) $2\%_{Au/Ag}$ (the trace labeled c10× is spectrum c magnified 10 times). All of the samples were concentrated to the same total gold concentration of 0.05 mM. (right) TEM images corresponding to spectra a, b, and c. All scale bars are 50 nm.

deposited gold was less than ca. $10\%_{Au/Ag}$, the deposited gold wires became so thin that upon dissolution of the silver template, the frames either shrank to reach a minimal critical nanowire size of 1.6−1.8 nm (when the deposited gold amount was larger than $1.5-2\%_{Au/Ag}$) or disintegrated into smaller rod fragments for the smallest amount of deposited gold (below ca. $1.5\%_{Au/Ag}$). The frame shrinkage can be rationalized in terms of the very high surface tension of the thin gold frames and the metal plasticity, consistent with the significantly lower melting points of nanostructures.

The gold frames prepared under the optimal conditions started to lose their continuity and structural integrity only at $1\%_{Au/Ag}$ (Figure 1h), where the thickness of the frame skeleton decreased below the critical size of ca. 1.6 nm (ca. 5 atomic diameters of gold). This size is similar to that of ultrathin gold nanostructures prepared by direct reduction of gold salts using oleylamine.[21] This size is also at the boundary of the metal-to-superatom transition for gold nanostructures.[29] With a skeleton thickness below the critical size for plasmons,[29] dispersions of thin frames ($2-4\%_{Au/Ag}$) in aqueous solution displayed low-intensity and relatively featureless spectra throughout the visible and near-IR (NIR) regions (Figure 4, spectra c and c10×). The weaker peaks in the thin-frame absorption were noticeable only in the 300−500 nm range, consistent with subplasmonic gold clusters.[29] At the same time, for the thicker gold frames (starting with ca. $7\%_{Au/Ag}$), there was an apparent IR absorption (Figure 4, spectrum a; also see Figure S5), consistent with plasmonic gold shell behavior.[12] The IR absorbance was relatively featureless because of the relative nonuniformity of the frames[22] and the complex geometry of the decahedral framework.

The crystallinity of the frames was confirmed by STEM nanodiffraction (Figure 2b) and the observation of the lattice fringes of the thicker portions of the frames (Figure S6). EDX showed that the frames are composed of 85−90 atom % gold (Figures S7 and S8), with the residual silver likely being in the form of a surface oxide.[27] In addition, we realized that at lower peroxide concentrations (ca. 0.05 M), a significant amount of silver can either be left undissolved or possibly redeposited back by the action of the residual ascorbic acid. Up to 60 atom % silver could be retained in the frames while essentially preserving their shape with some deterioration and roughness (Figure S9). Thus, tuning of the composition of the frames to some extent is possible, which may be useful for potential catalytic applications. The resulting alloying likely takes place upon silver dissolution and redeposition rather than upon the original gold deposition onto the AgNPs. The evidence of minimal alloying and gold diffusion during the deposition stage was corroborated by comparison of the frames produced by silver dissolution immediately after deposition and after 5 days (Figure S10), where no significant difference in frame quality could be observed.

We further explored similar gold deposition using different silver morphologies, including a mixture of cubes and bipyramids, silver platelets, and pentagonal rods.[30] None of those structures yielded comparable ultrathin frames. Notably, the gold deposition on the (111) pentagonal caps of the pentagonal rods resulted in well-defined frames, while the deposition on (100) facets was fairly uniform across the facets, leading to a porous mesh even at low $X\%_{Au/Ag}$ (Figure 5a,b). Preliminary investigations with silver icosahedra also demonstrated for this morphology the formation of gold frames bound exclusively by (111) facets arranged with pentagonal symmetry (Figure 5c). Overall, the success of ultrathin nanostructure formation for morphologies with pentagonal twinning emphasizes the importance of the presence of well-defined (111) planes joined at obtuse angles. The selective deposition along edges of such (111) facets can be rationalized by their relative stability resulting from the passivation with citrate. Consequently, the edges of (111) facets become preferred locations for deposition, whereas (100) facets are more reactive and gold deposition onto them proceeds more uniformly, resulting in cages and shells that have been well-explored for cubes.[7]

The ultrathin frames did not display SERS enhancement in solution at 785 nm excitation. No frame fluorescence could be detected either. Future work will be directed toward testing the

dx.doi.org/10.1021/ja111642d | J. Am. Chem. Soc. 2011, 133, 8066–8069

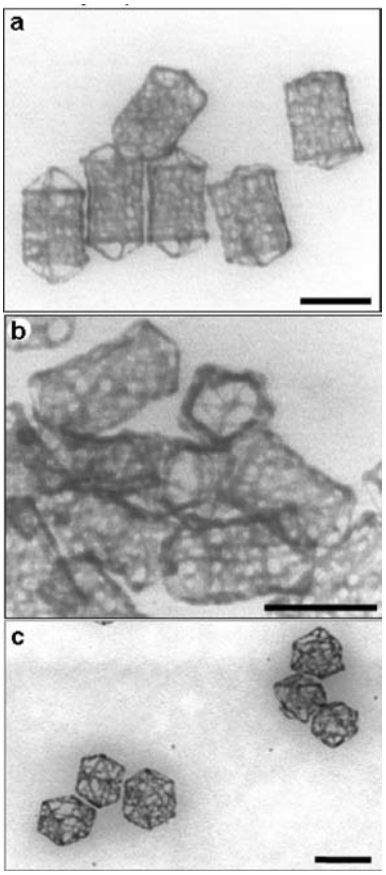

Figure 5. TEM images illustrating the formation of gold nanoframe structures templated from (a, b) faceted pentagonal silver nanorods and (c) icosahedra. All scale bars are 50 nm.

catalytic properties of these ultrathin gold nanostructures. At present we have obtained promising results for oxidative catalysis using the gold frames within a titania dispersion, though their activity is lower that that of gold−palladium nanoparticles[31] (see the SI for more details). This suggests that formation of the frames with platinum and palladium should be explored. Overall, the reported findings present a reliable procedure for the formation of ultrathin gold nanoframes with thicknesses as low as 1.6 nm by templating with pentagonal silver morphologies. The demonstrated approach can provide a viable complementary route to lithographic procedures for the formation of ultrathin metal nanostructures.

■ ASSOCIATED CONTENT

Supporting Information. Experimental protocols, additional electron microscopy images, and spectroscopic data. This material is available free of charge via the Internet at http://pubs.acs.org.

■ AUTHOR INFORMATION

Corresponding Author
vkitaev@wlu.ca

■ ACKNOWLEDGMENT

The authors thankfully acknowledge financial support by NSERC, CFI, and ORF-RI. V.K. is grateful to the Government of Ontario for the ERA Award. Andrew Frank is acknowledged for assistance with catalysis experiments.

■ REFERENCES

(1) Xia, Y. N.; Xiong, Y.; Lim, B.; Skrabalak, S. E. *Angew. Chem, Int. Ed.* **2009**, *48*, 60.
(2) Sau, T. K.; Rogach, A. L.; Jaeckel, F.; Klar, T. A.; Feldmann, J. *Adv. Mater.* **2010**, *22*, 1805.
(3) Yao, J.; Le, A.; Gray, S. K.; Moore, J. S.; Rogers, J. A.; Nuzzo, R. G. *Adv. Mater.* **2010**, *22*, 1102.
(4) Jain, P. K.; El-Sayed, M. A. *Chem. Phys. Lett.* **2010**, *487*, 153.
(5) Mulvihill, M. J.; Ling, X. Y.; Henzie, J.; Yang, P. *J. Am. Chem. Soc.* **2010**, *132*, 268.
(6) Giljohann, D. A.; Seferos, D. S.; Daniel, W. L.; Massich, M. D.; Patel, P. C.; Mirkin, C. A. *Angew. Chem., Int. Ed.* **2010**, *49*, 3280.
(7) Chen, J.; Yang, M.; Zhang, Q.; Cho, E. C.; Cobley, C. M.; Kim, C.; Glaus, C.; Wang, L. V.; Welch, M. J.; Xia, Y. N. *Adv Funct. Mater.* **2010**, *20*, 3684.
(8) Somorjai, G. A.; Li, Y. *Top. Catal.* **2010**, *53*, 832.
(9) Joo, S. H.; Park, J. Y.; Tsung, C.-K.; Yamada, Y.; Yang, P.; Somorjai, G. A. *Nat. Mater.* **2009**, *8*, 126.
(10) (a) Goubet, N.; Ding, Y.; Brust, M.; Wang, Z. L.; Pileni, M.-P. *ACS Nano* **2009**, *3*, 3622. (b) Sau, T. K.; Rogach, A. L. *Adv. Mater.* **2010**, *22*, 1781.
(11) (a) Sun, Y. G.; Xia, Y. N. *Science* **2002**, *298*, 2176. (b) Sun, Y. G.; Xia, Y. N. *Nano Lett.* **2003**, *3*, 1569.
(12) Skrabalak, S. E.; Chen, J.; Sun, Y.; Lu, X.; Au, L.; Cobley, C. M.; Xia, Y. N. *Acc. Chem. Res.* **2008**, *41*, 1587.
(13) Sun, Y.; Wiley, B.; Li, Z. Y.; Xia, Y. N. *J. Am. Chem. Soc.* **2004**, *126*, 9399.
(14) (a) Métraux, G. S.; Cao, Y. C.; Jin, R.; Mirkin, C. A. *Nano Lett.* **2003**, *3*, 519–522. (b) Au, L.; Chen, Y.; Zhou, F.; Camargo, P.; Lim, B.; Li, Z.; Ginger, D. S.; Xia, Y. N. *Nano Res.* **2008**, *1*, 441.
(15) (a) Rodríguez-González, B.; Burrows, A.; Watanabe, M.; Kiely, C.; Liz Marzán, L. M. *J. Mater. Chem.* **2005**, *15*, 1755. (b) Prevo, B. G.; Esakoff, S. A.; Mikhailovsky, A.; Zasadzinski, J. A. *Small* **2008**, *4*, 1183. (c) Aherene, D.; Gara, M.; Kelly, J. M.; Gun'ko, Y. K. *Adv. Funct. Mater.* **2010**, *20*, 1329.
(16) Okazaki, K.; Yasuia, J.; Torimoto, T. *Chem. Commun.* **2009**, 2917.
(17) Mahmoud, M. A.; El-Sayed, M. A. *J. Am. Chem. Soc.* **2010**, *132*, 12704.
(18) Mahmoud, M. A.; El-Sayed, M. A. *Nano Lett.* **2009**, *9*, 3025.
(19) Liusman, C.; Li, S.; Chen, X.; Wei, W.; Zhang, H.; Schatz, G. C.; Boey, F.; Mirkin, C. A. *ACS Nano* **2010**, *4*, 7676.
(20) Cademartiri, L.; Ozin, G. A. *Adv. Mater.* **2009**, *21*, 1013.
(21) (a) Huo, Z.; Tsung, C.; Huang, W.; Zhang, X.; Yang, P. *Nano Lett.* **2008**, *8*, 2041. (b) Lu, X.; Yavuz, M. S.; Tuan, H.; Korgel, B. A.; Xia, Y. N. *J. Am. Chem. Soc.* **2008**, *130*, 8900. (c) Li, Z.; Tao, J.; Lu, X.; Zhu, Y.; Xia, Y. *Nano Lett.* **2008**, *8*, 3052. (d) Wang, C.; Hu, Y.; Lieber, C. M.; Sun, S. *J. Am. Chem. Soc.* **2008**, *130*, 8902.
(22) Walter, M.; Akola, J.; Acevedo, O. L.; Jadzinsky, P. D.; Calero, G.; Ackerson, C. J.; Whetten, R. L.; Gronbeck, H.; Hakkinen, H. *Proc. Natl. Acad. Sci. U.S.A.* **2008**, *105*, 9157.
(23) Pietrobon, B.; Kitaev, V. *Chem. Mater.* **2008**, *20*, 5186.
(24) Jana, N.; Gearheart, L.; Murphy, C. J. *Chem. Commun.* **2001**, 617.
(25) Ma, Y.; Li, W.; Cho, E. C.; Li, Z.; Yu, T.; Zeng, J.; Xie, Z.; Xia, Y. *ACS Nano* **2010**, *4*, 6725.
(26) Sun, Y. G.; Xia, Y. N. *J. Am. Chem. Soc.* **2004**, *126*, 3892.
(27) Zhang, Q.; Cobley, C. M.; Zeng, J.; Wen, L. P.; Chen, J.; Xia, Y. N. *J. Phys. Chem. C* **2010**, *114*, 6396.
(28) Lu, X.; Au, L.; McLellan, J.; Li, Z. Y.; Marquez, M.; Xia, Y. N. *Nano Lett.* **2007**, *7*, 1764.
(29) Jin, R. *Nanoscale* **2010**, *2*, 343.
(30) Pietrobon, B.; McEachran, M.; Kitaev, V. *ACS Nano* **2009**, *3*, 21.
(31) Frank, A. J.; Rawski, J.; Maly, K. E.; Kitaev, V. *Green Chem.* **2010**, *12*, 1615.